Regional Pulmonary Perfusion in Patients with Acute Pulmonary Edema

Daniel P. Schuster, MD[1,2]; Claire Anderson, MD[2]; James Kozlowski, MS[2]; and Neale Lange, MD[1]

[1]*Department of Medicine, Washington University School of Medicine, St. Louis, Missouri; and* [2]*Department of Radiology, Washington University School of Medicine, St. Louis, Missouri*

Redistribution of pulmonary blood flow (PBF) away from edematous regions of the lung is characteristic of experimental acute lung injury (ALI), helping to preserve ventilation–perfusion matching and gas exchange. The purpose of this study was to determine if such perfusion redistribution occurs in acute pulmonary edema in humans. **Methods:** We measured the regional distribution of lung water concentration (LWC) and PBF with PET in 9 patients with ALI, 7 patients with non-ALI pulmonary edema, and 7 healthy subjects. **Results:** The average patient chest radiographic score was 7.5 ± 2.2 (scale: 0–12, where ≥4 met our criterion for pulmonary edema). The mean partial pressure of oxygen, arterial/fraction of inspired oxygen ratio ($Pa_{O_2}/F_{I_{O_2}}$) was 192 ± 78. LWC was 35 ± 4 mL H_2O/100 mL lung versus 20 ± 5 mL H_2O/100 mL lung in the healthy subjects ($P < 0.05$). On average, the ventral-to-dorsal regional distribution of PBF was similar in patients with pulmonary edema and healthy subjects, regardless of the etiology of the pulmonary edema. However, LWC and an index of perfusion redistribution away from edematous lung regions, when combined, were a significant determinant of the $Pa_{O_2}/F_{I_{O_2}}$ (coefficient of determination [R^2] = 0.53; $P = 0.03$). **Conclusion:** These results suggest that hypoxic vasoconstriction is severely blunted in ALI. The perfusion redistribution that does exist contributes slightly to improved oxygenation during early pulmonary edema in humans.

Key Words: respiratory distress syndrome, adult; CT, emission; pulmonary edema; pulmonary gas exchange

J Nucl Med 2002; 43:863–870

A defining characteristic of acute lung injury (ALI) and the acute respiratory distress syndrome (ARDS) is severe hypoxemia. This gas exchange abnormality is the result of noncardiogenic pulmonary edema, atelectasis, cell infiltration and debris in the alveolar compartment, and bronchoconstriction. All of these factors affect ventilation of lung units. However, gas exchange is ultimately determined by the matching of regional perfusion with regional ventilation. Unfortunately, little information is available about how regional perfusion is affected in patients with ALI/ARDS. In animal models of ALI, perfusion is almost always reduced to edematous lung regions. Thus, the regional pattern of pulmonary blood flow (PBF) is an important determinant of gas exchange, and interventions that alter the perfusion pattern in response to regional edema accumulation cause serious additional disturbances in oxygenation (*1–3*).

It has been recognized for some time that mild-to-moderate pulmonary hypertension is frequently present during the initial stages of ALI/ARDS (*4–6*). Factors contributing to this increase in pulmonary vascular resistance include vasoconstriction (from alveolar hypoxia or biochemical mediators), vascular obstruction (microthrombosis or endothelial cell swelling), and vascular compression (from edema). The relative importance of each of these factors in ALI/ARDS is unknown. Several studies have described the nature and extent of the disturbance in ventilation–perfusion matching with the multiple inert-gas elimination technique (*7,8*). However, the only direct, spatially oriented, measurements of regional PBF in humans with ALI/ARDS were obtained previously with the relatively low-resolution technique of γ-scintigraphy with radiolabeled macroaggregates and could not be correlated with simultaneous measurements of the distribution of pulmonary edema (*9*).

PET has been used extensively in animal models to study the relationships between regional pulmonary perfusion and pulmonary edema (*10*). In this study, we used PET to better define the relationship between regional pulmonary perfusion and lung water accumulation in patients with both ALI and non-ALI forms of pulmonary edema. We wanted to determine whether the pattern of perfusion redistribution regularly identified in animal models of ALI (*1–3*) also occurs in humans.

MATERIALS AND METHODS

Subjects

We studied 16 patients with pulmonary edema and 7 healthy volunteers. Patients were selected if they met radiographic criteria for pulmonary edema, regardless of the underlying cause or the degree of hypoxemia, and could be studied <72 h from the onset of developing pulmonary infiltrates. Patients were excluded if they

Received Aug. 8, 2001; revision accepted Feb. 21, 2002.

For correspondence or reprints contact: Daniel P. Schuster, MD, Pulmonary and Critical Care Division, Washington University School of Medicine, 660 S. Euclid Ave., University Box 8225, St. Louis, MO 63110-1093.

E-mail: schusted@msnotes.wustl.edu

or their physician declined participation, if they required a fraction of inspired oxygen (F_{IO_2}) of >0.7 to maintain an arterial saturation of >90% by finger pulse oximetry, or if they had hemodynamic or cardiac rhythm instability during the 6 h before scanning. Patients were subsequently classified and analyzed as having ALI/ARDS if they met radiographic criteria for acute pulmonary edema as just described and had a documented clinical cause for ALI. In the absence of an appropriate risk factor for ALI, they were classified as non-ALI/ARDS. This classification scheme is in accord with the American–European Consensus Conference definitions for ALI/ARDS (*11*).

This study was approved by the Washington University School of Medicine Human Studies Committee and by the Radioactive Drug Research Committee. All patients or their families gave informed consent.

Chest Radiographic Evaluation

We identified patients with pulmonary edema from portable chest radiographs, using a previously reported protocol (*12*). Each patient met all 3 of the following criteria: a chest radiographic score of ≥4, involvement of basilar and perihilar regions bilaterally at a minimum, and at least 1 region on each side with a score of ≥2.

To score the radiograph, each lung was divided into apical, perihilar, lateral, and inferior regions. Each region was then evaluated separately on a scale of 0–3: 0 = no infiltrate, 1 = minimal or barely perceptible infiltrate, 2 = moderate interstitial infiltrate but without obscuration of pulmonary vessels, and 3 = extensive confluent infiltrate with or without air bronchograms that obscured pulmonary vessels. The highest possible score within a region was used (e.g., the entire region did not have to be involved uniformly to achieve a score of 3). Each lung was scored separately, and the scores for each lung were summed. Then the total scores of each lung were averaged. Thus, the final total score could range from 0 to 12.

PET

PET scans were obtained using an ECAT EXACT HR Plus 962 scanner (Siemens/CTI, Knoxville, TN), a 63-plane positron camera with an axial sampling of 2.43 mm, isotropic resolution 4.6 mm, and a 15 × 56 cm field of view (FOV). To improve the signal-to-noise ratio of the activity measurements, we reduced the data to 10 slices by combining 6 original planes to form a single transverse slice with an axial sampling of 15 mm.

PET scanning consisted of transmission and $H_2{}^{15}O$ emission scans. The transmission scan was obtained with a linear rod source of $^{68}Ge/^{68}Ga$ over a 15-min acquisition period. This scan was used to correct subsequent emission data for attenuation effects and also to provide images of lung and chest density that were used to define regions of interest (ROIs) on the lung images. Methods associated with using this radiopharmaceutical to measure regional pulmonary flow and lung water in humans have been described (*13*) and summarized (*10*).

Subjects lay in the supine position. A venous cannula was inserted into a forearm vein for tracer infusion. Arterial blood pressure, electrocardiography, and O_2 saturation were monitored throughout the study.

Next, approximately 1,895 MBq (50 mCi) $H_2{}^{15}O$ were injected in 2 fractions into a forearm vein. Approximately 948 MBq (25 mCi) of activity were first injected by hand over a 10-s period. Activity data were collected at the start of the injection for 60 s in list mode. The distribution of this activity in the lungs is proportional to the regional PBF. At the end of this period, the second fraction of activity (~569 MBq [15 mCi] after decay) was injected as a bolus. Then 4 min after the initial injection, a second PET data collection was started to determine the apparent regional partition coefficient for the tracer (necessary for calculation of PBF) (*10*).

Image Analysis

ROIs for the lung were drawn on the transmission images (Fig. 1). Each ROI included all lung image elements on each side of the

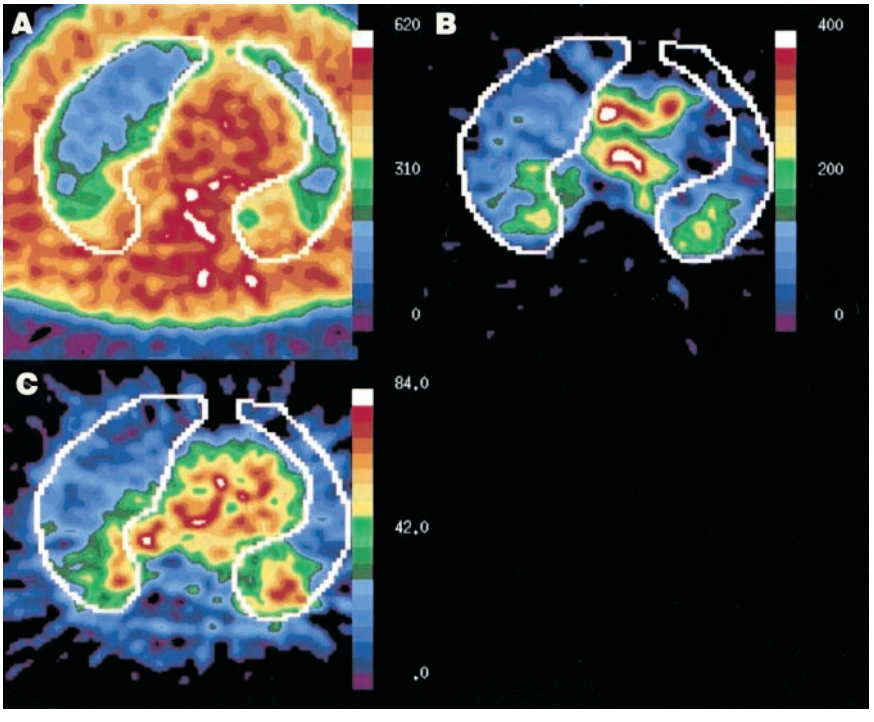

FIGURE 1. Sample PET images from patient PH226 (Table 1) with pulmonary edema. (A) Transmission image. Scale is in arbitrary units, where higher numbers indicate greater attenuation of activity (i.e., greater tissue density). Scan is comparable with typical CT scan, except with approximately 1/10th the spatial resolution. Scan is used to identify lung regions (white outlines). (B) PBF image. Units are mL/min/100 mL lung. (C) Lung water concentration (LWC) image. Units are mL H_2O/100 mL lung. Normal upper limits for LWC by these methods are approximately 25 mL H_2O/100 mL lung. Note dorsal predominance of lung water accumulation. Also note general concordance between regional blood flow and lung water distributions (i.e., there is no appreciable perfusion redistribution away from regions of increased LWC [pulmonary edema]).

thorax for that image. The hila, chest wall, and diaphragm were excluded from such regions. Typically, ROIs were drawn on 6 of 10 planes with the most lung pixels. These 6 slices were contiguous.

Images for PBF were processed as described (*13*). The list mode data from the initial 60 s were processed into consecutive 3-s frames. Beginning with the first frames showing a significant increase in activity in the FOV (Fig. 2), a set of 6 consecutive frames (18 s) was combined into a single image. This composite image was used to calculate PBF according to the following equation:

$$C_{PET} = C_i\lambda(T_2 - T_1 - [e^{k_1} - e^{k_2}]\lambda/PBF), \qquad \text{Eq. 1}$$

where $k_2 = (T_2 \cdot PBF)/\lambda$, $k_1 = (T_1 \cdot PBF)/\lambda$, C_{PET} is the PET-measured regional tissue activity (cpm/100 mL lung) (cpm = counts per minute), C_i is the input concentration of tracer in blood perfusing the lung (cpm/100 mL blood), λ is the regional tissue–blood partition coefficient for water ([mL lung water/mL lung]/[mL blood water/mL blood]), T_1 = time of scan start (s) and T_2 = time of scan stop (s), and PBF is measured in mL/min/100 mL lung. Note that the denominator "mL lung" in each case includes the contents of vascular, extravascular, and alveolar (air) compartments.

ROIs from the right and left lungs were defined on each transmission scan. The first frames of activity after injection of $H_2{}^{15}O$ were also used to locate and generate a right ventricular cavity ROI. The mean value for activity within this latter region was used to generate the input function in Equation 1. Because activity within the right ventricle precedes activity in lung tissue regions, the first frame used to define the input function was also defined as the first frame to show a significant increase in activity in the right ventricular ROI. In other words, the 6 frames used to calculate the lung tissue activity and the 6 frames used to calculate the input function were not always the same, but might be offset by 1 or 2 frames, depending on the delay of activity reaching the lung from the right ventricle (Fig. 2).

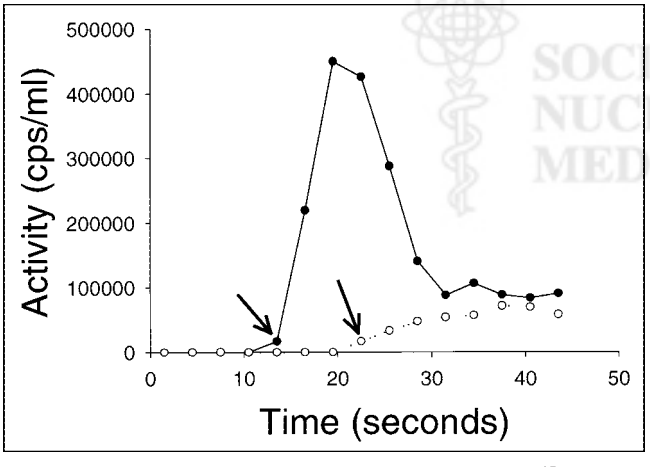

FIGURE 2. Time–activity data after injection of $H_2{}^{15}O$ in patient PH226 (Table 1). Each point represents data from 3-s scan. Arrows point to first frame used to determine beginning of composite 18-s scan formed to estimate PBF from Equation 1. Note delay in activity reaching lung tissue region (○) from right ventricle (●). cps = counts per second.

The position of each region was kept in the computer memory, and mean values for each region were obtained for all PET measurements. To normalize the regional PBF data for differences in cardiac output, PBF in each picture element (pixel) was expressed as a fraction of the total blood flow to the region.

To evaluate the relationship of PBF to anatomic position within a region, the *x*- and *y*-coordinates for each pixel, along with the respective fractional PBF values for each pixel, were recorded. The pixel data were then sorted, first by their *y*-coordinate. Next, within each value for *y*, the data were sorted again by their *x*-coordinate. The result was a listing of the pixels by location, beginning in the most ventral-to-medial portion of the region and ending with the most dorsal-to-lateral portion of the region. Each region contained approximately 400–500 pixels. Arbitrarily, the data were divided into 20 bins that were stacked vertically in the ventral-to-dorsal direction, so each bin contained approximately 20–25 pixels, which could then be averaged. By keeping the number of bins per region and the number of tomographic slices per subject constant, bin values could be averaged across subjects, allowing comparisons between experimental groups. The mean PBF for each region was expressed in units of mL blood/min/100 mL lung.

Statistical Methods

Data are presented as the mean ± SD. Differences between means were analyzed for statistical significance by an unpaired *t* test. Relationships between variables were analyzed by standard linear regression techniques. All statistical analyses were performed with SigmaStat 2.0 (SPSS, Inc, Chicago, IL).

RESULTS

Patient characteristics are given in Table 1. Nine patients were classified as ALI/ARDS and the remainder were classified as non-ALI/ARDS (in general, congestive heart failure, volume overload due to renal failure, and so forth). As might be expected, the ALI/ARDS patients were treated more often with antibiotics ($P = 0.07$) than the non-ALI/ARDS patients, but the non-ALI/ARDS patients were treated more often with aspirin ($P = 0.02$) and angiotensin-converting enzyme inhibitors ($P = 0.07$) than the ALI/ARDS patients. Importantly, vasodilators were not being used by the ALI/ARDS patients at the time of the imaging study.

In 13 (intubated) patients (in whom the F_{IO_2} could be measured accurately), the partial pressure of oxygen, arterial/F_{IO_2} (Pa_{O_2}/F_{IO_2}) was 192 ± 78. The Pa_{O_2}/F_{IO_2} of the ALI/ARDS group alone was nearly identical (191 ± 82). The average chest radiographic score was 7.5 ± 2.2 (scale: 0–12, where a score of 4 met our criterion for pulmonary edema). The average score in the ALI/ARDS group (8.0 ± 2.6) was higher than that in the non-ALI/ARDS group (6.9 ± 1.6), but this difference was not statistically significant. Four of the 16 patients eventually died during the hospitalization, 2 in each clinical subgroup.

Although mechanical ventilatory support was not standardized in this study, the clinicians caring for these patients followed current guidelines relating to the importance of pressure-targeted ventilation (*14*). Accordingly, peak air-

TABLE 1
Clinical Information About Patients with Pulmonary Edema

Patient ID	Sex	Age (y)	Diagnosis	Pao_2/FIo_2	CXR score	Outcome
Non-ALI/ARDS						
PH211	F	42	Chronic renal failure	141	6.5	D
PH212	F	60	Congestive heart failure	NA	9.5	A
PH228	F	66	Chronic renal failure	NI	4.5	A
PH229	M	63	Chronic renal failure	NI	8	A
PH230	F	32	Congestive heart failure	NI	5.5	A
PH233	M	40	Chronic renal failure	288	7	D
PH234	F	71	Congestive heart failure	158	7	A
ALI/ARDS						
PH224	F	70	Leukemia/sepsis	102	8.5	A
PH226	F	65	Influenza, acute MI	89	5.5	A
PH232	F	78	Bilateral pneumonia	253	5	A
PH236	F	47	Leukemia/sepsis	235	4	A
PH250	F	75	Eosinophilic pneumonia	203	8.5	D
PH251	F	50	Septic cholangitis	107	10	D
PH258	M	45	Sepsis	332	9.5	A
PH259	F	60	Sepsis	232	9	A
PH271	M	42	Aspiration	168	12	A

ID = identification; Pao_2/FIo_2 = partial pressure of oxygen, arterial/fraction of inspired oxygen; CXR score = chest radiographic score; D = died; NA = not available; A = alive at hospital discharge; NI = not intubated; MI = myocardial infarction.

way pressures were always <30 cm H_2O by the time of the day of the imaging study, and the positive end-expiratory pressure (PEEP) ranged between 5 and 10 cm H_2O. Patients with more severe disturbances in gas exchange requiring even greater levels of mechanical ventilatory support generally did not meet our criteria for clinical stability for transfer to the PET imaging facility.

Seven new healthy subjects were also studied, including 2 women (age, 28–41 y). To improve the robustness of these normal data, the data were combined with previously reported data from 6 other healthy subjects (*13*). No significant difference was found between the data from the 2 groups of healthy subjects.

The average lung water concentration (LWC) from all regions from all patients with pulmonary edema was significantly greater than that in healthy subjects (Fig. 3). No significant difference was found between the 2 patient groups. Likewise, the LWC in patients with pulmonary edema was greater in all pixel bins along the ventral-to-dorsal axis (Fig. 4). No significant correlation was found between the average LWC (Fig. 3) and the chest radiographic score (Table 1).

The mean PBF (proportional to cardiac output) in patients with pulmonary edema was similar to that measured in healthy subjects (Fig. 5). Likewise, the regional distribution of PBF along the ventral-to-dorsal axis in patients with pulmonary edema was within 1 SD of the spatial distribution measured in healthy subjects (Fig. 6). There was a trend for patients with non-ALI/ARDS to have less perfusion to dorsal (gravity dependent) lung regions than patients with ALI/ARDS, but this difference was not statistically significant. Of the 16 patients, only 4 showed a distribution that was outside the normal distribution shown in Figure 6 (data not shown). Two of these patients had non-ALI/ARDS acute pulmonary edema after missing regularly scheduled hemodialysis (i.e., most likely consistent with volume overload), and 2 had pulmonary edema associated with systemic infection (i.e., consistent with ALI/ARDS).

The relationship of perfusion distribution to lung water distribution is shown in Figure 7 by combining the data from Figures 4 and 6. The rightward shift in the curves from the patient groups is the result of the increase in LWC (i.e., pulmonary edema). However, the distributions of perfusion within the distribution of pulmonary edema are virtually identical (i.e., no perfusion redistribution).

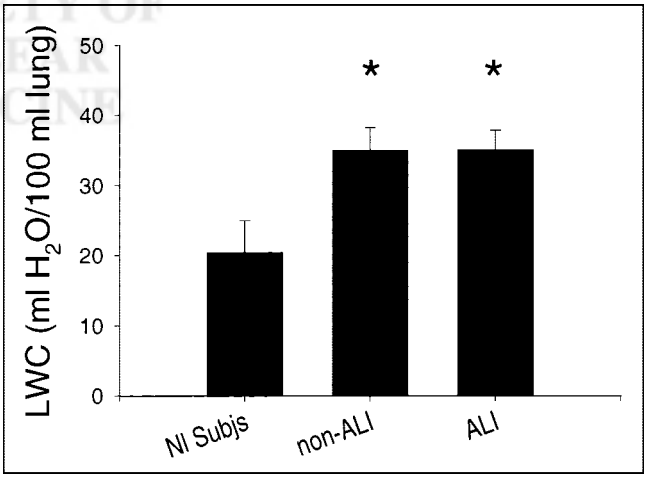

FIGURE 3. LWC in healthy (normal) subjects (NI Subjs) (n = 12) and patients with ALI/ARDS (ALI) (n = 9) or non-ALI/ARDS (n = 7) pulmonary edema. *$P < 0.05$

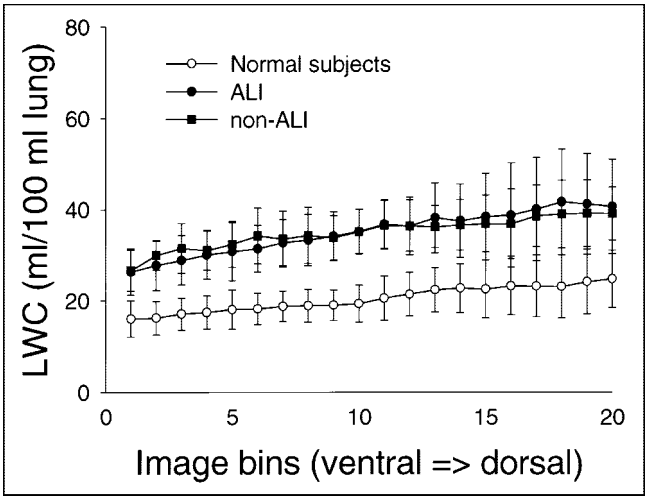

FIGURE 4. Regional distribution of LWC in healthy (normal) subjects (Nl Subjs) and patients with ALI/ARDS (ALI) or non-ALI/ARDS (non-ALI) pulmonary edema. Data are taken from PET images after sorting picture elements (pixels) into bins along ventral-to-dorsal axis. LWC in all bins from patients was significantly greater than that in healthy subjects.

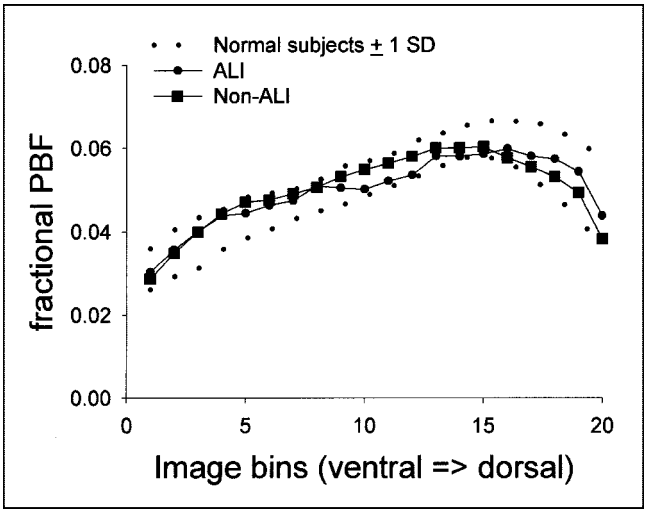

FIGURE 6. Regional distribution of fractional PBF in healthy (normal) subjects and patients with pulmonary edema (ALI and Non-ALI). Data are taken from PET images after sorting picture elements (pixels) into bins along ventral-to-dorsal axis. PBF data have been normalized for differences in cardiac output among individuals by dividing value for PBF in each pixel by mean PBF for same tomographic slice. For clarity of presentation, only mean values for PBF in pulmonary edema patients are shown. These values lie within ±1 SD of comparable values for healthy subjects (i.e., on average, distributions are not significantly different).

We define perfusion redistribution as a reduction in regional PBF (i.e., reduced fractional PBF in a given pixel bin) in an area of pulmonary edema. To quantify perfusion redistribution, when and if it occurred, we summed the fractional PBF data from the most dorsal one third of image bins ($fPBF_{14-20}$) (Fig. 6) (i.e., the bins with the greatest concentration of lung water (Fig. 4). In 12 patients with pulmonary edema who required mechanical ventilatory support (and thus, in whom we could accurately determine the Pa_{O_2}/F_{IO_2} at the time of PET), we determined the relationship between the Pa_{O_2}/F_{IO_2} as the dependent variable and the average LWC (Fig. 4) and $fPBF_{14-20}$ (Fig. 6) as the independent variables. Both variables together contributed significantly to the following linear regression relationship: $Pa_{O_2}/F_{IO_2} = 937 - (6.6 \cdot LWC) - (12 \cdot fPBF_{14-20})$. The coefficient of determination (R^2) was 0.53 (i.e., 53% of the

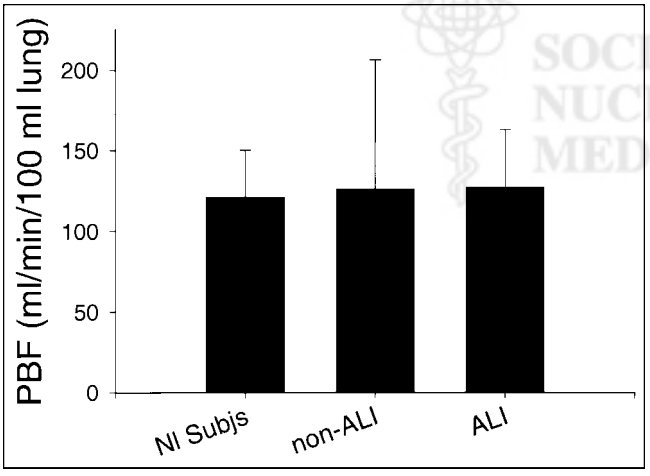

FIGURE 5. Mean PBF, which is proportional to cardiac output, as estimated from PET of healthy (normal) subjects (Nl Subjs) and patients with ALI/ARDS (ALI) or non-ALI/ARDS (non-ALI) pulmonary edema. No significant difference was found between the 2 groups.

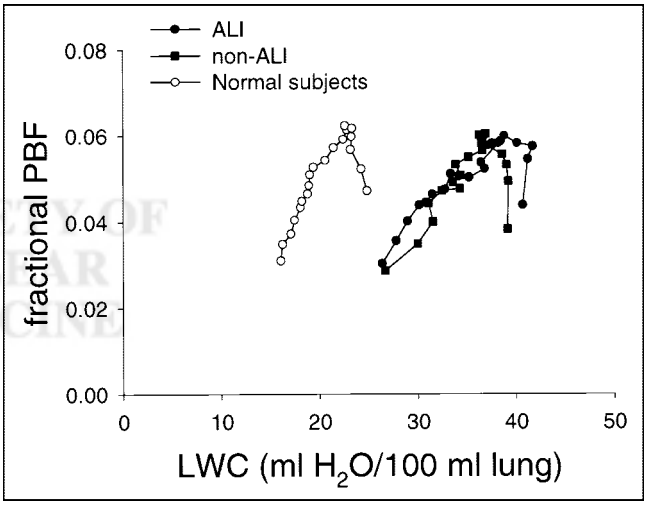

FIGURE 7. Regional distribution of fractional PBF in healthy (normal) subjects and patients with pulmonary edema (ALI and non-ALI) versus LWC. Data represent combination of data from Figures 4 and 6. Each symbol represents 1 image bin. For clarity of presentation, only mean values are shown. Rightward shift of curves from pulmonary edema patients represents increase in LWC (i.e., pulmonary edema). However, PBF distributions within each LWC distribution are nearly identical (i.e., there is no perfusion redistribution in patients with pulmonary edema compared with pattern seen in healthy subjects).

variation in Pa_{O_2}/F_{IO_2} was explained by the 2 independent variables). *P* for the overall regression was 0.032; probability values for contributions by LWC and $fPBF_{14-20}$ were 0.016 and 0.048, respectively.

An example of PET images from 1 patient with pulmonary edema (patient PH226; Table 1) is shown in Figure 1.

DISCUSSION

The main finding of this study is that the regional pulmonary perfusion pattern in patients with moderate-to-severe pulmonary edema is not, on average, significantly different from that measured in healthy subjects. This finding is distinctly different from the pattern of perfusion redistribution that is regularly observed in animal models of ALI, using the same or similar techniques to evaluate PBF and topographic perfusion patterns (*2*,*15*–*17*). Accordingly, mechanisms that might maintain more normal ventilation–perfusion matching, by redistributing blood flow away from areas of lung edema (such as hypoxic pulmonary vasoconstriction [HPV]), appear to be severely blunted in early human pulmonary edema. This observation appears to be true regardless of the underlying cause of pulmonary edema (i.e., either ALI/ARDS or non-ALI/ARDS). However, some small, although perhaps at times clinically significant, amounts of perfusion redistribution may still be present because we also found that the perfusion pattern together with the amount of pulmonary edema is a significant determinant of gas exchange. To our knowledge, these data are the first to actually reveal the spatial distribution of PBF in patients with pulmonary edema and its potential impact on oxygenation.

It has been known for several decades that pulmonary hypertension of varying severity is virtually universal in patients with ALI/ARDS (*5*). Although it is generally accepted that multiple causes are responsible for the increase in pulmonary arterial pressure, the role of HPV is of special interest, because HPV could act as a homeostatic control mechanism to reduce perfusion to low ventilation–perfusion (V/Q) lung units, thereby improving gas exchange (*18*). However, documenting the importance or even presence of HPV in ALI/ARDS is not easy because the exact mechanism of HPV remains unknown (*6*). Thus, the role of HPV in ALI/ARDS must necessarily be evaluated inferentially.

The existing data relating to the effectiveness of HPV in ALI/ARDS are conflicting. Zapol et al. (*5*) have reasoned that, because hypoxemia per se can worsen pulmonary pressures in ALI/ARDS, HPV is probably intact. Similarly, numerous studies have documented that vasodilators of various sorts cause gas exchange to deteriorate (*19*–*21*), implying that some vasoactive mechanism that was protecting gas exchange had been inhibited. On the other hand, some vasoconstrictors are known to enhance oxygenation in ALI/ARDS (*22*–*24*), strongly suggesting that pulmonary vessels, at least in areas of reduced ventilation, were not optimally vasoconstricted, possibly because of an ineffective HPV. This latter type of observation is consistent with experimental data in animal models that suggest that HPV is blunted in ALI (*3*) or is unlikely to be particularly effective even if, nevertheless, intact (*25*).

None of the studies in humans has been able to directly evaluate the regional pattern of PBF per se. In the current study, direct measurements of regional PBF showed little overall change from the normal pattern (Figs. 6 and 7), despite the presence of significant increases in pulmonary edema (Figs. 3, 4, and 7) and moderate-to-severe hypoxemia (Table 1).

We have recently reported that the most likely mechanism for perfusion redistribution in at least one commonly used experimental model of lung injury is HPV (*26*). Thus, given the lack of evidence for perfusion redistribution in patients with pulmonary edema in our study, a reasonable inference is that HPV, or any similar vasoactive mechanism, is severely blunted. However, because we also found that oxygenation was significantly dependent on the magnitude of edema accumulation (quantified as LWC) and on an index of perfusion redistribution ($fPBF_{14-20}$), some degree of local vasoconstriction may still be present. Thus, overall, these observations are consistent with studies cited previously of vasodilators and vasoconstrictors in ALI/ARDS that show deleterious and salutary effects on oxygenation, respectively. Interestingly, we found no indication that the lack of perfusion redistribution was characteristic of patients with ALI/ARDS as opposed to other causes of pulmonary edema. This last conclusion must be tempered by the imprecision that unfortunately is present in making clinical distinctions between ALI/ARDS and other causes of pulmonary edema (*27*).

We know of only one previous study that actually measured regional pulmonary perfusion in patients with ALI/ARDS per se. Pistolesi et al. (*9*) used classic perfusion lung γ-scintigraphy after radiolabeled albumin macroaggregates or microsphere administration in 19 patients with ALI/ARDS. However, only 13 patients were studied during the initial 72 h of their illness, as in our study. Although this study documented frequent perfusion defects, it is not possible to discern whether there was any significant perfusion redistribution compared with the normal pattern or compared with the distribution of lung water accumulation. Furthermore, others have failed to find scintigraphic evidence for perfusion redistribution during pulmonary edema secondary to congestive heart failure (as we confirmed with PET in this study) (*28*).

Our results are consistent with a recent study using the multiple inert-gas elimination technique that showed little change in the dispersion of PBF in patients with ALI in response to breathing 100% oxygen, although arterial oxygenation did deteriorate (*29*). Indeed, the multiple inert-gas elimination technique has been used in previous studies to show the relationship between ventilation and perfusion in ALI (*7*,*8*). These studies have shown, in general, that hypoxemia was predominantly due to intrapulmonary shunting

(as opposed to perfusion to regions of very low ventilation–perfusion ratios). Santos et al. (*29*) speculated that their results were consistent with absorption atelectasis, instead of any significant effect on HPV, and such a result would be expected if HPV was already severely blunted and perfusion redistribution was not present. However, from a study of the ventilation–perfusion distributions alone, it is impossible to know whether changes in regional perfusion (redistribution) occurred because of improved ventilation without any change in regional perfusion, because of a physical redistribution of perfusion to better ventilated lung units, or some combination of these 2 factors. Such conclusions require direct measurements of regional pulmonary perfusion.

If HPV (or any other similar compensatory mechanism) is blunted in acute pulmonary edema, what might be the mechanism? One interesting possibility is suggested by several recent studies from our laboratory (*1*,*2*,*26*). In the oleic acid model of ALI, at least, HPV seems to be not only intact but also quite effective in preserving gas exchange. However, we have also found that small doses of endotoxin—doses that themselves have little intrinsic hemodynamic effects—act synergistically with ALI to markedly increase the production of prostacyclin. The net effect is a complete ablation of HPV and a marked deterioration in oxygenation. Whether this or a similar mechanism is operative in human forms of ALI/ARDS is unknown.

Some limitations to our study should be noted. We were only able to study patients who were clinically stable enough for transport to the PET imaging facility. By necessity, we excluded patients with the most severe forms of respiratory failure associated with acute pulmonary edema. It seems unlikely to us that as patients become more ill and gas exchange deteriorates further, we would find that perfusion redistribution would become more manifest as a compensatory mechanism. Nevertheless, without being able to make these measurements directly, we cannot be certain.

At our center, pulmonary artery catheterization is not routinely performed for ALI/ARDS. Thus, we were not able to correlate our observations about a pulmonary perfusion pattern with classic measurements of hemodynamics. For the same reason, we cannot be certain that the clinical classification of patients into the subgroups of ALI/ARDS and non-ALI/ARDS were the results of pure increased permeability edema, on the one hand, and pure increased hydrostatic pressure pulmonary edema on the other. Indeed, overlap is common. Importantly, the patients with ALI/ARDS were not receiving known vasodilators at the time of the imaging study.

We also were unable to perform these studies under conditions of standardized mechanical ventilation. However, the clinicians caring for these patients followed current guidelines concerning pressure-targeted ventilation (*11*). Accordingly, peak airway pressures were always <30 cm H_2O, and PEEP ranged between 5 and 10 cm H_2O. Again, it seems unlikely that we would have observed more perfusion redistribution among patients who required even greater levels of airway pressure support because studies in canine models of ALI show that PEEP reverses perfusion redistribution (*30*).

Finally, the spatial resolution of PET and our units (bins) for image analysis are considerably larger than the acinar gas exchange unit. However, in animal studies, this scale of imaging is still able to detect significant changes in the perfusion pattern that correlate with changes in gas exchange (*1*,*2*). It is precisely these changes in the perfusion pattern that were not observed in humans in the current study and that are so striking in their difference from the observed pattern in animals.

CONCLUSION

Our data suggest that compensatory vasoactive mechanisms responsible for perfusion redistribution and the relative preservation of ventilation–perfusion matching, such as hypoxic vasoconstriction, are severely blunted in patients with acute pulmonary edema. Nevertheless, the perfusion redistribution that does exist contributes slightly to improved oxygenation. Pharmacologic interventions that can further enhance this effect without increasing pulmonary capillary pressures might be a useful new therapeutic strategy in such patients.

ACKNOWLEDGMENT

This research was supported in part by National Institutes of Health grant HL32815.

REFERENCES

1. Gust R, McCarthy TJ, Kozlowski J, et al. The response to inhaled nitric oxide in acute lung injury depends on the distribution of pulmonary blood flow prior to its administration. *Am J Respir Crit Care Med.* 1999;159:563–570.
2. Gust R, Kozlowski J, Stephenson AH, et al. Synergistic hemodynamic effects of low-dose endotoxin in acute lung injury. *Am J Respir Crit Care Med.* 1998;157:1919–1926.
3. Leeman M, Delcroix M, Vachiery JL, et al. Blunted hypoxic vasoconstriction in oleic acid lung injury: effect of cyclooxygenase inhibitors. *J Appl Physiol.* 1992;72:251–258.
4. Zapol W, Snider M. Pulmonary hypertension in severe acute respiratory failure. *N Engl J Med.* 1977;296:476–480.
5. Zapol W, Rie M, Frikker M, et al. Pulmonary circulation during adult respiratory distress syndrome. In: Zapol W, Falke W, eds. *Acute Respiratory Failure: Lung Biology in Health and Disease.* New York, NY: Marcel Dekker; 1985:241–274.
6. Romand J, Donald F, Suter P. Cardiopulmonary interactions in acute lung injury: clinical and prognostic importance of pulmonary hypertension. *New Horiz.* 1994;2:457–462.
7. Dantzker D, Brook C, DeHart P, et al. Ventilation-perfusion distributions in the adult respiratory distress syndrome. *Am Rev Respir Dis.* 1979;120:1039–1052.
8. Ralph D, Robertson H, Weaver L, et al. Distribution of ventilation and perfusion during positive end-expiratory pressure in the adult respiratory distress syndrome. *Am Rev Respir Dis.* 1985;131:54–60.
9. Pistolesi M, Miniati M, Di Ricco G, et al. Perfusion lung imaging in the adult respiratory distress syndrome. *J Thorac Imaging.* 1986;1:11–24.
10. Schuster D. The evaluation of lung function with PET. *Semin Nucl Med.* 1998;28:341–351.
11. Bernard G, Artigas A, Brigham K, et al. The American-European Consensus Conference on ARDS: Definitions, Mechanisms, Relevant Outcomes, and Clinical Trial Coordination. *Am J Respir Crit Care Med.* 1994;149:818–824.
12. Anderson D, Glazer H, Semenkovich J, et al. Lung transplant enema: chest radiography after lung transplantation—the first ten days. *Radiology.* 1995;195:275–281.

13. Schuster DP, Kaplan JD, Gauvain K, et al. Measurement of regional pulmonary blood flow with PET. *J Nucl Med.* 1995;36:371–377.
14. Network TARDS. Ventilation with lower tidal volumes as compared with traditional tidal volumes for acute lung injury and the acute respiratory distress syndrome. *N Engl J Med.* 2000;342:1301–1308.
15. Sprague RS, Stephenson AH, Dahms TE, et al. Effect of cyclooxygenase inhibition on ethchlorvynol-induced acute lung injury in dogs. *J Appl Physiol.* 1986;61:1058–1064.
16. Sprague RS, Stephenson AH, Dahms TE, et al. Effects of ibuprofen on the hypoxemia of established ethchlorvynol-induced unilateral acute lung injury in anesthetized dogs. *Chest.* 1987;92:1088–1093.
17. Gust R, Stephenson A, McCarthy T, et al. Role of cyclooxygenase-2 in oleic acid-induced acute lung injury. *Am J Respir Crit Care Med.* 1999;160:1165–1170.
18. Fishman A. Hypoxia on the pulmonary circulation: how and where it acts. *Circ Res.* 1976;38:221–231.
19. Radermacher P, Santak B, Wust H, et al. Prostacyclin for the treatment of pulmonary hypertension in the adult respiratory distress syndrome: effects on pulmonary capillary pressure and ventilation-perfusion distributions. *Anesthesiology.* 1990;72:238–244.
20. Melot C, Lejeune P, Leeman M, et al. Prostaglandin E1 in the adult respiratory distress syndrome: benefit for pulmonary hypertension and cost for pulmonary gas exchange. *Am Rev Respir Dis.* 1989;139:106–110.
21. Radermacher P, Santak B, Becker H, et al. Prostaglandin E1 and nitroglycerin reduce pulmonary capillary pressure but worsen ventilation-perfusion distributions in patients with adult respiratory distress syndrome. *Anesthesiology.* 1989; 70:601–606.
22. Reyes A, Roca J, Rodriguez-Roisin R, et al. Effect of almitrine on ventilation-perfusion distribution in adult respiratory distress syndrome. *Am Rev Respir Dis.* 1988;137:1062–1067.
23. Reyes A, Lopez-Messa J, Alonso P. Almitrine in acute respiratory failure: effects on pulmonary gas exchange and circulation. *Chest.* 1987;91:388–393.
24. Prost J, Desche P, Jardin F, et al. Comparison of the effects of intravenous almitrine and positive end-expiratory pressure on pulmonary gas exchange in adult respiratory distress syndrome. *Eur Respir J.* 1991;4:683–687.
25. Grant BJB, Davies EE, Jones HA, et al. Local regulation of pulmonary blood flow and ventilation-perfusion ratios in the coatimundi. *J Appl Physiol.* 1976;40:216–228.
26. Brimioulle S, Julien V, Gust R, et al. Importance of hypoxic vasoconstriction in maintaining oxygenation during experimental acute lung injury [abstract]. *Am J Respir Crit Care Med.* 2001;163:A452.
27. Schuster DP. What is acute lung injury? What is ARDS? *Chest.* 1995;107:1721–1726.
28. Newman G, Sullivan D, Gottschalk A, et al. Scintigraphic perfusion patterns in patients with diffuse lung disease. *Radiology.* 1982;143:227–231.
29. Santos C, Ferrer M, Roca J, et al. Pulmonary gas exchange response to oxygen breathing in acute lung injury. *Am J Respir Crit Care Med.* 2000;161:26–31.
30. Schuster DP, Howard DK. The effect of positive end-expiratory pressure on regional pulmonary perfusion during acute lung injury. *J Crit Care.* 1994;9:100–110.